Journal of Engineering Physics and Thermophysics, Vol. 75, No. 5, 2002

SOME REGULARITIES OF HEAT AND MASS TRANSFER IN THE CASE OF FIRE WITHIN A BUILDING

S. V. Puzach and V. M. Kazennov

UDC 614.841.4

Results of a numerical investigation of heat and mass transfer at the initial stage of fire within a building in combustion of kerosene, carried out with the use of a three-dimensional mathematical field model, are presented. A comparison of the distribution of the averaged temperatures and velocities along the vertical axis of the convective column and of the mass rates of gas flows through an open opening with the experimental data has been made. Substantial three-dimensional inhomogeneities of the velocities and the temperatures in the near-ceiling layer have been revealed. It has been established that near the opening there is a critical separation zone which influences significantly the parameters of natural gas transfer.

1. Among emergencies of different types, fires rank first in Russia in the number of people's deaths [1]. Every year, about 300,000 fires occur in the country, and the level of traumatism and losses in people as a result of these fires is the highest in the world — it is about three times larger than that in other developed countries.

The actual physicochemical processes occurring during the fire are complex nonstationary three-dimensional heat- and mass-transfer processes that are not clearly understood. The accuracy and reliability of the method of calculation of heat and mass transfer play a key part in providing for the safety of people, selecting the parameters and sites of disposition of fire detectors and explosion safety systems, and realizing efficient fire-prevention measures. It is difficult to devise such a method because of the multifactoredness and nonlinearity of the problem. Mathematical modeling of turbulent heat and mass transfer under complex gasdynamic and thermal conditions (including combustion within a building) is among the thirty most important and interesting problems of physics, determined by the Russian Academy of Sciences for the next few years [2], and further accumulation of theoretical and experimental data on the regularities of heat and mass transfer in the case of fire is a pressing problem.

2. To investigate the regularities of heat and mass transfer in the case of fire within a building, a three-dimensional mathematical field model described in detail in [3, 4] is used. The following main simplifications of the actual thermogasdynamic picture of the process are introduced:

a) the gas medium in the building is locally thermodynamically and chemically equilibrium;

b) the gas medium is a mixture of ideal gases and smoke (solid particles);

c) the velocities and the temperatures of the components of the gas mixture are equal at each point of the space;

d) the chemical reaction of combustion is single-stage and irreversible;

e) the dissociation and ionization of the medium as well as the thermal and pressure diffusion of the gases are negligibly small;

f) turbulent pulsations have no influence on the thermophysical properties of the medium;

g) the mutual influence of turbulence and radiation is insignificant.

The nonstationary three-dimensional differential equations of the laws of conservation of mass, momentum, and energy are solved for the gas medium of the building (Navier–Stokes equations in Reynolds form) and for the components of the gas medium and the optical density of the smoke. All of them are reduced to the "standard" form [5] suitable for numerical solution:

$$\frac{\partial}{\partial \tau}(\rho \Phi) + \operatorname{div}(\rho w \Phi) = \operatorname{div}(\Gamma \operatorname{grad} \Phi) + S\,, \tag{1}$$

Academy of State Fire-Prevention Service, Moscow, Russia; email: puzachsv@hotmail.com. Translated from Inzhenerno-Fizicheskii Zhurnal, Vol. 75, No. 5, pp. 130–137, September–October, 2002. Original article submitted January 15, 2002; revision submitted April 9, 2002.

1062-0125/02/7505-1165$27.00

TABLE 1. Parameters and Coefficients of Eq. (1)

Φ	Γ	S
1	0	G_m
w_x	$\mu + \mu_c$	$\frac{\partial}{\partial x}\left(\Gamma \frac{\partial w_x}{\partial x}\right) + \frac{\partial}{\partial y}\left(\Gamma \frac{\partial w_y}{\partial x}\right) + \frac{\partial}{\partial z}\left(\Gamma \frac{\partial w_z}{\partial x}\right) - \frac{\partial p}{\partial x} - \frac{2}{3}\frac{\partial}{\partial x}(\Gamma \operatorname{div} w)$
w_y	$\mu + \mu_t$	$\frac{\partial}{\partial x}\left(\Gamma \frac{\partial w_x}{\partial y}\right) + \frac{\partial}{\partial y}\left(\Gamma \frac{\partial w_y}{\partial y}\right) + \frac{\partial}{\partial z}\left(\Gamma \frac{\partial w_z}{\partial y}\right) - \frac{\partial p}{\partial y} - \frac{2}{3}\frac{\partial}{\partial y}(\Gamma \operatorname{div} w)$
w_z	$\mu + \mu_t$	$\frac{\partial}{\partial x}\left(\Gamma \frac{\partial w_x}{\partial z}\right) + \frac{\partial}{\partial y}\left(\Gamma \frac{\partial w_y}{\partial z}\right) + \frac{\partial}{\partial z}\left(\Gamma \frac{\partial w_z}{\partial z}\right) - \frac{\partial p}{\partial z} - \frac{2}{3}\frac{\partial}{\partial x}(\Gamma \operatorname{div} w) - \beta g \Delta T$
X_{O_2}	$(D_{O_2} + D_{O_{2t}})\rho$	$-L_{O_2}\psi\eta$
X_{CO}	$(D_{CO} + D_{CO_t})\rho$	$L_{CO}\psi\eta$
X_{CO_2}	$(D_{CO_2} + D_{CO_{2t}})\rho$	$L_{CO_2}\psi\eta$
k	μ_t/σ_k	$\nu_t\left(\frac{\partial w_j}{\partial x_i}\left(\frac{\partial w_i}{\partial x_j} + \frac{\partial w_j}{\partial x_i}\right) + \frac{g}{\mathrm{Pr_t}}\frac{1}{T}\frac{\partial T}{\partial z}\right) - \varepsilon$
ε	μ_t/σ_ε	$C_1\frac{\varepsilon}{k}\nu_t\left(\frac{\partial w_j}{\partial x_i}\left(\frac{\partial w_i}{\partial x_j} + \frac{\partial w_j}{\partial x_i}\right) + \frac{g}{\mathrm{Pr_t}}\frac{1}{T}\frac{\partial T}{\partial z}\right) - C_2\frac{\varepsilon^2}{k}$
W	0	$W_{sp}\psi$
i	$\lambda + \lambda_t + \lambda_r$	$\psi\eta Q_w^{low} - Q_r + \mu\,\Phi_{dis}$

where Φ is a dependent variable, Γ is the diffusion coefficient for Φ, and S is the source term. All the values presented here and hereafter are time-averaged. The parameters and coefficients of Eq. (1) are presented in Table 1.

The k–ε model of turbulence with the following set of empirical constants [6] is used: $C_1 = 1.44$, $C_2 = 1.92$, $\sigma_k = 1.0$, $\sigma_\varepsilon = 1.3$, and $C_\mu = 0.09$. The effective values in Eq. (1) are represented in the following form: $\mu_{eff} = \mu + \mu_t$, $\lambda_{eff} = \lambda + \lambda_t + \lambda_r$, and $D_{eff} = D + D_t$.

The dynamic viscosity of the gas is determined from the Sutherland formula [6] and the turbulent viscosity is determined from the Kolmogorov formula [6]. The turbulent thermal conductivity is calculated from the relation $\lambda_t = c_p \mu_t/\mathrm{Pr_t}$, and the turbulent diffusion is calculated from $D_t = \mu_t/\rho \mathrm{Pr_d}$. It is assumed that $\mathrm{Pr_t} = \mathrm{Pr_d} = 1$ [6].

In calculating radiative heat transfer in the gas medium, we use the approximation of an optically thin layer [7] since below we will perform numerical investigation of heat and mass transfer at the initial stage of fire, for which the optical density of the medium outside the flame is low [1]. In this case, we have $\lambda_r = 0$ in the energy equation, and the internal heat sink is determined from the formula [7]

$$Q_r = 4\pi\gamma\sigma_r T^4 . \tag{2}$$

The integral emissivity of the gas γ in Eq. (2) is equal [8] to

$$\gamma = 1 - \exp(-\theta\delta) . \tag{3}$$

The coefficient of attenuation of the radiation is determined from the calculated optical density of the smoke [8]:

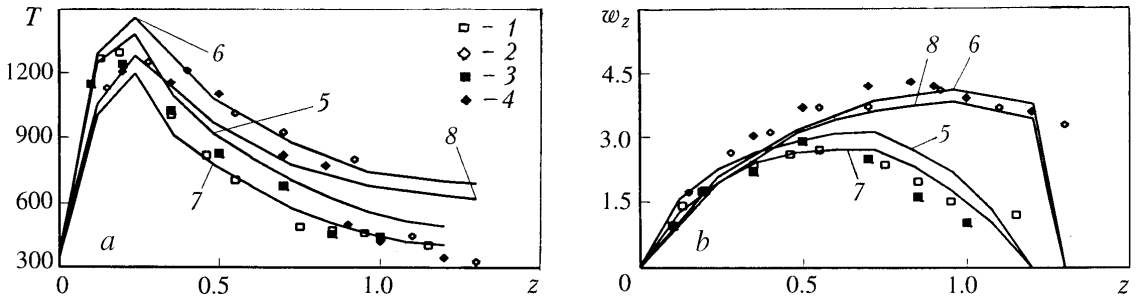

Fig. 1. Distribution of the averaged temperatures (a) and of the projections of the averaged velocity on the vertical axis (b) along the axis of the convective column in combustion: acetone: 1, 2) experiment [9] and 5, 6) calculation; butanol: 3, 4) experiment [9] and 7, 8) calculation. T, K. w_z, m/sec; z, m.

$$\theta = \lambda^* W . \tag{4}$$

The rate of gasification of the liquid combustible material is equal [8] to

$$\psi = \psi_{sp} F_c \sqrt{\tau / \tau_{stab}} . \tag{5}$$

In stabilized combustion ($\tau \geq \tau_{stab}$), $\psi = \psi_{sp} F_c$.

The rate of release of the optical density of the smoke from the surface of the combustible material is determined as in [8]:

$$W = W_{sp} \psi . \tag{6}$$

The combustion region is specified by the volume sources of mass and heat, distributed uniformly over the volume of the parallelepiped with a base equal to the area of the open surface of the combustible material and a height of $h = 2a_c$. The completeness of combustion is assumed to be such as in a fire outdoors [8]. It is assumed that outside this region there is no after-burning of the gasified combustible material. This assumption is true at the initial stage of the fire where the oxidizer is present in excess.

It is assumed that in the parts of the computational region which are occupied by enclosing structures the effective coefficient of thermal conductivity is equal to the coefficient of thermal conductivity of the material of the enclosing structures and the effective viscosity is $\mu_{eff} = 10^{10}$ kg/(m·sec). Thus, the condition $w_x = w_y = w_z = 0$ is provided inside the solid material, which allows one to solve Eq. (1) by continuous calculation over the entire computational region without separating the internal solid boundaries.

The boundary conditions for Eq. (1) are assumed to be as follows:

a) on the inner surfaces of the enclosing structures, the projections of the velocities are equal to zero; for the energy equation, boundary conditions of the third kind are set (experimental values of the heat-transfer coefficients presented in [3, 8]); for the other parameters, $\partial\Phi/\partial n = 0$;

b) in the plane of the cross section of an open opening or at the conditional boundaries of the adjacent region of the outside air, we have $\partial\Phi/\partial n = 0$ in the region of flow of the gas outward through these boundaries; in the region of flow of the outside air inward, the pressure, the temperature, and the concentrations of the components correspond to the atmospheric-air parameters.

The initial conditions (at $\tau = 0$ sec) have the following form: $T = T_0$, $p = p_0$, $w_x = w_y = w_z = 0$, $G_{fl.g} = G_{ent.a} = 0$, $X_{O_2} = 0.23$, $X_{N_2} = 0.77$, $X_{CO} = X_{CO_2} = 0$, and $W = 0$.

Equation (1) is solved by the control-volume method [5] according to the implicit finite-difference scheme on a uniform staggered grid. For this purpose, the equation for a pressure correction in "contractible" form is used. The distribution of the gas-medium parameters inside each control volume is assumed to be corresponding to the upwind difference scheme. The time step is determined from the Courant condition [5].

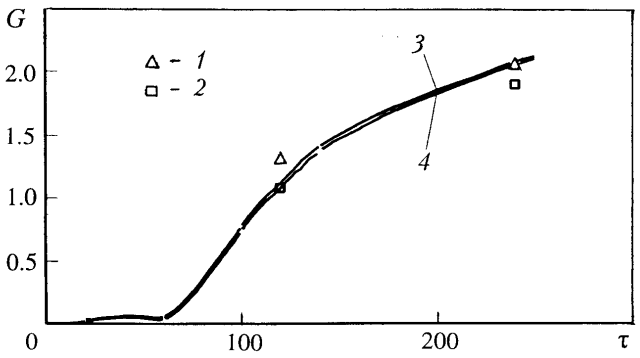

Fig. 2. Mass rates of hot gas flows outward and of outside-air flows inward through the opening vs. time in combustion of wood: $G_{fl.g}$: 1) experiment [11], 3) calculation; $G_{ent.a}$: 2) experiment [11], 4) calculation. $G_{fl.g}$, $G_{ent.a}$, G, kg/sec; τ, sec.

The results of the calculation by the model proposed, obtained on 11 × 11 × 11 and 21 × 21 × 21 finite-difference grids with time steps of $5 \cdot 10^{-4}$ and 10^{-5} sec at different Courant numbers [5], differed from each other by no more than 5%. Moreover, the accuracy of the calculations was controlled by the fulfillment of the local and integral laws of conservation of mass and energy in the computational region.

3. The results of the comparison of the calculated distribution of the averaged temperatures and the projections of the averaged velocity on the vertical axis along the central axis of the convective column formed above the combustion source with the experimental data [9] are presented in Fig. 1. A stabilized combustion of two combustible liquids — acetone and butanol — is considered.

The finite-difference grid had dimensions 21 × 21 × 11. The region of the building of length 6 m and width 6 m, adjacent to the combustion source, was included into the computational region. Curves 1, 2, 5, and 6 in Fig. 1 have been obtained at d_c = 0.2 m, while curves 3, 4, 7, and 8 have been obtained at d_c = 0.4 m. The rate of gasification of the fire load in the case of stabilized combustion was assumed to be equal to ψ_{sp} = 0.044 kg/(sec·m^2) for acetone and ψ_{sp} = 0.033 kg/(sec·m^2) for butanol [10]. The other physicochemical properties necessary for calculation were determined according to [10].

The calculation error did not exceed 20% for the temperature and 25% for the velocity projection as compared to the experimental data.

A comparison of the results of the calculation of the mass rates of hot-gas flows outward and of outside-air flows inward through the open openings with the experimental data [11] is presented in Fig. 2. The combustible material (wood) is positioned at the center of the building with dimensions 5.8 × 5.8 × 5.8 m with two open openings.

In the experiment [11], the mass flow rates were measured in the vertical symmetry plane of the openings; this being so, the inhomogeneity of the velocity and temperature fields in the openings, which was very marked (analogous results have been obtained in [4]), is not included in the experimental results. The difference between the calculation and the experiment did not exceed 19%.

A comparison with other experimental data and analytical solutions obtained by the field model proposed has been made in [3, 4, 12].

4. The initial data of the numerical experiment were assumed to be as follows:

a) the dimensions of the building, as for the inner surfaces of the enclosion structures, were 6 × 6 × 3 m, and the dimensions of the entire computational region with the outside-air region adjacent to the opening were 12 × 6 × 6 m;

b) the upper cut of one open opening with dimensions 0.6 × 1 or 0.6 × 2, positioned symmetrically relative to the wall, was at the level of the ceiling;

c) the combustible material was kerosene of mass M = 50 kg with the following parameters of the process of its gasification [10]: ψ_{sp} = 0.05 kg/(sec·m^2), Q_w^{low} = 43.54 MJ/kg, W_{sp} = 249 Np·m^2/kg, L_{CO} = 0.148, L_{CO_2} = 2.92; L_{O_2} = 3.34, τ_{stab} = 1 sec, Bu = θd_{eff}, and $d_{eff} = \sqrt{4F_c/\pi}$; the absorption coefficient and the emissivity of the flame were determined from the Bu number using experimental relations [8];

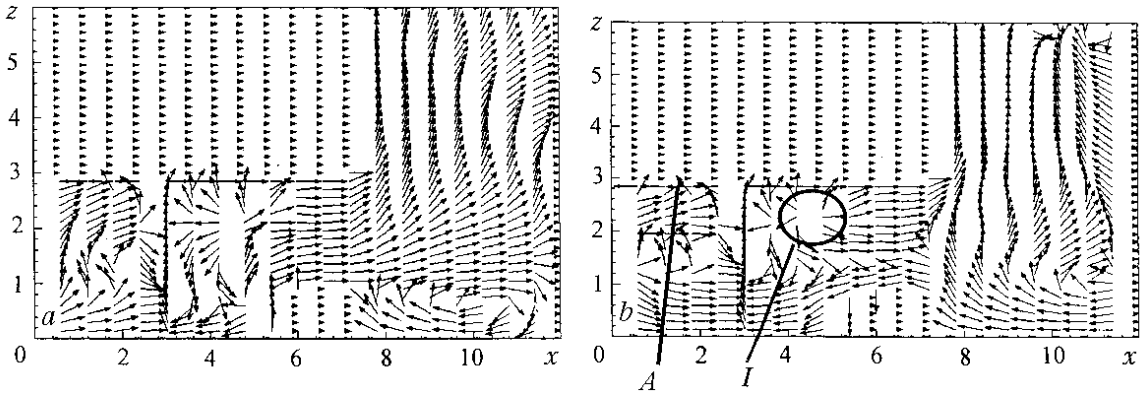

Fig. 3. Schemes of flow in the plane perpendicular to the floor after 10 (a) and 20 sec (b) from the beginning of combustion at the height of the opening H_{open} = 2 m: 1) critical zone. *x*, *z*, m.

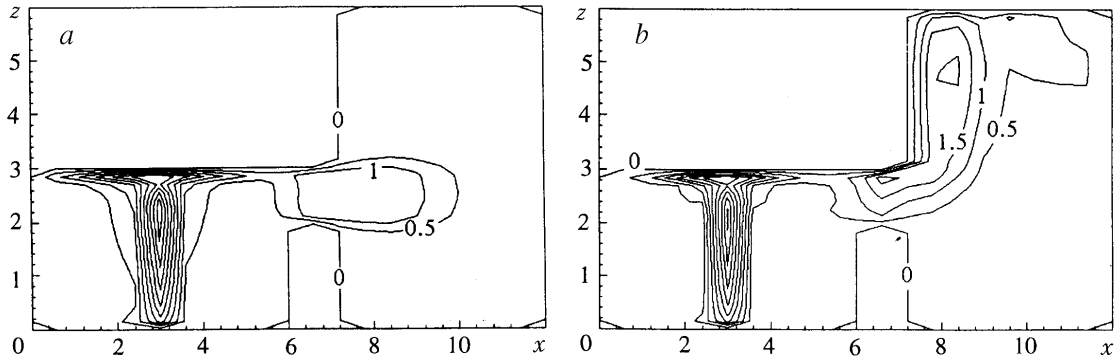

Fig. 4. Velocity fields in the plane perpendicular to the floor after 5 (a) and 20 sec (b) from the beginning of combustion at the height of the opening H_{open} = 1 m. *x*, *z*, m.

d) the area of the open surface of kerosene poured into a square vessel with a geometric center coincident with the center of the floor of the building was F_c = 0.36 m^2;

e) the atmospheric-state parameters were as follows: temperature 293 K, pressure 10^5 Pa, and velocity of the wind 0 m/sec.

The initial temperature of the gas medium in the building, of the enclosing structures, and of the outside air was assumed to be identical and equal to T_0 = 293 K. The temperature of the enclosing structures was assumed to be constant with time. The systems of mechanical ventilation, fire suppression, and heating were not used.

The uniform finite-difference computational grid had dimensions 21 × 11 × 41 (number of points). In this case, the step along the *x* and *y* axes was 0.6 m, the step along the *z* axis was 0.15 m, and the time step was 0.001 sec.

5. The calculation results show that the thermogasdynamic pattern of the flow is complex in character and it changes with time.

Figure 3 shows the schemes of flow in the plane which is perpendicular to the floor, passes through its geometrical center, and is in parallel to the length of the building, at different instants of time from the beginning of the combustion. The height of the opening was H_{open} = 2 m. The velocity fields in this plane (at H_{open} = 1 m) are shown in Fig. 4. The figures correspond to the value of the velocity expressed in meters per second.

It is clear from Figs. 3 and 4 that near the opening there is a stable critical zone of a retarded gas, which determines the gas transfer through the opening. The reason for the appearance of this zone is the action of the longitudinal positive pressure gradient on the boundary layer. The fields of the velocity projection on the *x* axis in the cross section parallel to the *y*0*z* plane and perpendicular to the floor and passing through the center of this region are shown in Fig. 5. At the point of separation of the laminar boundary layer on the surface of the span (point *A* in Fig.

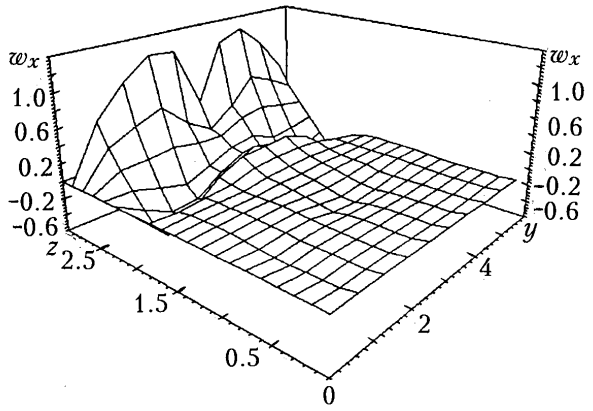

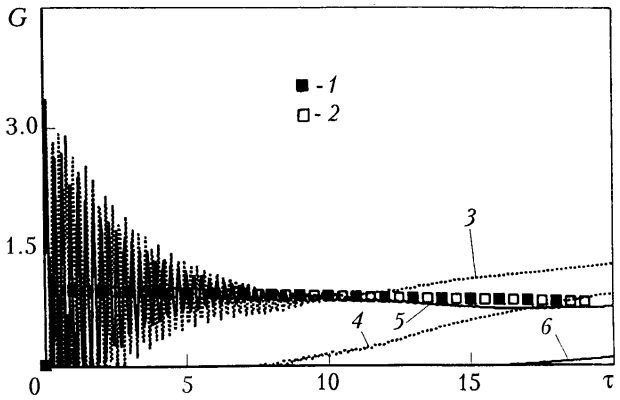

Fig. 5. Field of the velocity projection on the x axis in the cross section perpendicular ton the floor and passing through the center of the critical zone. w_x, m/sec; y, z, m.

Fig. 6. Mass rates of flows through the opening vs. time from the beginning of combustion: 1) analytical solution [14], 2) integral model [13] ($G_{\text{fl.g}}$), field model: $G_{\text{fl.g}}$: 3) H_{open} = 2 and 5) 1 m; $G_{\text{ent.a}}$: 4) 2 and 6) 1 m. G, kg/sec; τ, sec.

3) the condition $f\text{Re}^{**} = -0.089$ is fulfilled [6], which lends support to the correctness of the computational method used.

The calculations have shown that the dimensions of the revealed zone are independent of the height of the opening. If the height of this zone H_{zone}, equal to 1.2 m in this case, is larger than the height of the opening, the outside air does not enter through the opening ("choking" regime). In the case where $H_{\text{zone}} \le H_{\text{open}}$, after a certain time, the air begins to permeate into the building below this zone.

These results are illustrated in Fig. 6, which shows the dependences of the mass rates of gas flows through the opening on the time from the beginning of the combustion. The inflow of the outside air begins within 16.4 sec at a height of the opening of H_{open} = 1 m and within 7.5 sec at H_{open} = 2 m. At a smaller height, the critical zone breaks down at the moment when the air begins to enter, otherwise it continues to exist for a certain time and then breaks down.

It is clear from Fig. 4 that at the initial instants of time, for example, after 5 sec (Fig. 4a), the convective column formed above the site of compustion has the shape of a conventionally conal body broadening in the vertical direction, which corresponds to the commonly accepted notions of its shape in an infinite space (for example, [8]). However, the influence of the enclosing structures of the building results in the transverse dimension of the column decreasing when it approaches the surface of the span after a certain time (Fig. 4b).

The results obtained show that the development of zonal models for calculating the thermogasdynamics of a fire on the assumption that there is a uniformly heated unseparated jet gas layer near the ceiling requires additional substantiation for concrete conditions of the problem. For example, in combustion of ethanol on condition that the other initial data of the problem are the same no separation zone was formed on the ceiling. This is explained by the fact that the heat release was approximately two times smaller in this case than in combustion of kerosene [10]; therefore, the positive pressure gradients on the ceiling were much lower.

6. A comparison of the results of the calculation of the mass rates of flows through the opening, carried out by the field model proposed, with the results obtained using the integral model [13] and the results of the analytical solution [14] is presented in Fig. 6. It is clear from this figure that the pulsations of the mass rates (and of the pressure) of gas flows moving through the opening outward decay with time approximately within 10 sec. This does not mean that the finite-difference scheme used is unstable, since the local and integral laws of conservation of mass and energy are fulfilled with an error of no more than 5% throughout the computational region. The observation of actual fires [8] lends qualitative support to this fact.

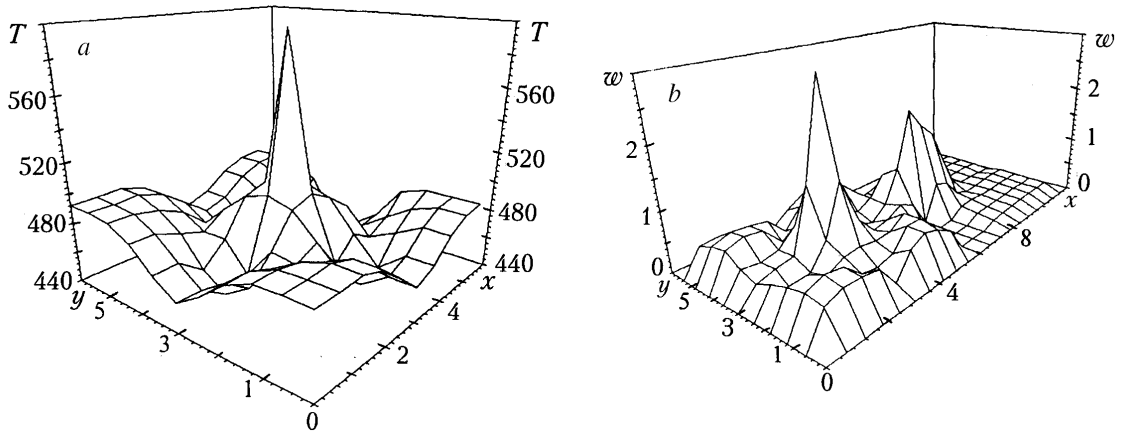

Fig. 7. Distributions of the temperatures (a) and the velocities (b) in the plane parallel to the floor and positioned at a distance of 0.15 m from the ceiling. *T*, K. *w*, m/sec; *x*, *y*, m.

The calculations made in [3] by this field model have revealed significant pressure pulsations and insignificant pulsations of the flow rate. This is explained by the fact that in this work the numerical experiment was carried out at a higher energy release: here t_{stab} = 1 sec, and in [3] τ_{stab} = 60 sec.

The time-averaged calculated values of the mass rate of gas flows moving outward, obtained by the model proposed (Fig. 6, curves 3 and 5), coincide with the analytical solution for the time of work done by the opening in releasing the gas outward with an error of no more than 5%. The difference is explained by the fact that the viscous dissipation of energy in the gaseous medium of the building is not taken into account in the analytical solution (and in the integral model).

The mass flow rates obtained by the integral model are practically coincident with the rates calculated in the analytical solution, since the latter is a particular case of it (the opening works only in releasing the gas outward [8]). The integral model does not point to the existence of the flow of the outside air inward within the time interval considered. This is confirmed by the fact that the "quasistationary" distributions of pressure along the height of the building inside and outside it are used in this model for calculating the natural gas transfer through the opening, and the internal pressure near the opening is determined from the volume-mean parameters [8]. However, the existence of the above-considered critical zone near the opening makes this assumption invalid, and the use of the integral model for calculating the initial stage of a fire (as, for example, in [15]) can lead, in some cases, to incorrect qualitative as well as quantitative results.

7. The calculation results point to significant inhomogeneities of the temperature, velocity, and concentration fields in the building, which cannot be revealed with the use of the integral, zonal, and two-dimensional field models of the thermodynamics of a fire. In [4, 16], the three-dimensional effects of heat and mass transfer inside the building and in the openings have been revealed without consideration of the adjacent region of outside air.

Figure 7 shows the distributions of the temperatures and the velocities over the plane parallel to the floor and positioned at a distance of 0.15 m from the span. It is clear from the figure that at the corners of the ceiling the gas mixture has higher temperature and velocity. The temperature in this cross section has a maximum on the axis of the convective column and four local maxima at the corners. The velocity field also has a maximum on the axis of the column, four local maxima at the corners, and two maxima in the throat cross section of the opening and at a height of 5 m outside the building (Fig. 4b), which is why the temperature sensors and detectors of the component or smoke concentration, positioned in different parts of the span, come into action at different instants of time.

When the size of the computational region changes to the dimensions of the building without the outside-air region adjacent to the opening (the boundary surfaces are the inner surfaces of the enclosing structures and the cross-sectional plane of the opening coincident with the plane of the inner surface of the wall), the parameters of heat and mass transfer are practically the same after 2.1 sec from the beginning of combustion. This is explained by the fact that before the instant of time τ = 2.1 sec the excess pressure (the difference between the local values of the gas pres-

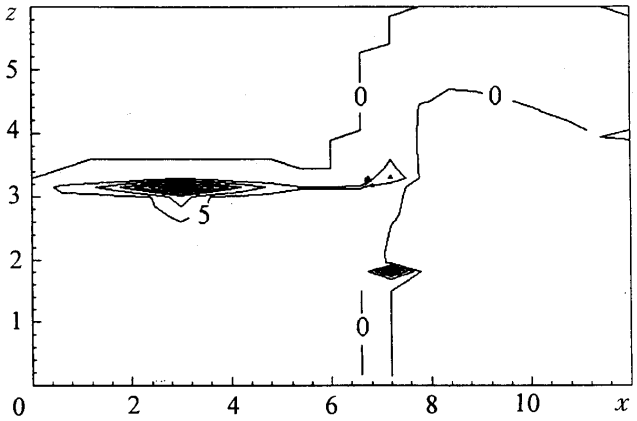

Fig. 8. Isobars in the plane perpendicular to the floor after 10 sec from the beginning of combustion.

sure and the atmospheric pressure at this height) on the inner plane of the opening depends on the time: for example, at τ = 0.5 sec $p = -25$ Pa, and at τ = 1 sec $p = -12$ Pa. After τ = 2.1 sec, the isobar with an excess pressure p = 0 (the pressure is equal to the atmospheric one) is practically coincident with this plane and then the pressure on it does not change with time.

This is confirmed by Fig. 8, which shows isobars in the plane perpendicular to the floor after 10 sec from the beginning of combustion. The figures correspond to the value of the excess pressure expressed in Pa. Thus, the boundary condition on an open opening (in the region of flow of the outside air inward, the pressure, the temperature, and the concentration of the components correspond to atmospheric-air parameters) is fulfilled exactly; therefore, the addition of the outside-air region in the case of combustion influences the accuracy of the calculation of the heat and mass transfer only during a negligibly small initial time interval.

Taking account of the additional hydraulic resistance of the opening in the presence of the adjacent region leads to a time delay in the beginning of the outside-air flow into the building. However, for the given initial data this time delay is insignificant (0.1 sec); therefore, the curves of the mass rates of flows through the opening (Fig. 5) are practically coincident in both variants.

CONCLUSIONS

1. The use of the integral and zonal mathematical models of the thermogasdynamics of a fire for calculating its initial stage can give qualitatively and quantitatively incorrect results in the case of formation of stable separation zones of a gas on the ceiling. Taking into account this phenomenon, one must refine the formulas used in these methods for calculating natural gas transfer through the opening.

2. The inclusion of the outside-air region adjacent to the opening in the absence of wind in the calculations has an insignificant influence on the parameters of heat and mass transfer within the building at the initial stage of the fire.

3. The new regularities of heat and mass transfer in the case of fire within a building, calculated on the basis of the numerical experiment, must be taken into account in developing recommendations on the safe evacuation of people and the placement of fire detectors.

NOTATION

T, temperature; ρ, density; p, pressure; τ, time; w, velocity; G, mass rate of the gas flow; c_p, specific heat at constant pressure; ψ, rate of gasification of the combustible material; x, y, z, coordinates along the length, width, and height of the building, respectively; γ, integral emissivity of the gas layer; δ, thickness of the gas layer; λ^*, coefficient for conversion of the optical radiation range to the infrared one; θ, coefficient of attenuation of radiation by a gas me-

dium of thickness δ; λ, μ, ν, and D, coefficients of molecular thermal conductivity, kinematic viscosity, dynamic viscosity, and diffusion, respectively; Pr and Pr_d, Prandtl number and diffusion Prandtl number; i, enthalpy; g, free-fall acceleration; k, kinetic energy of turbulence; ε, dissipation rate of the kinetic energy of turbulence; β, coefficient of volumetric thermal expansion; Q, volume internal energy source; Q_w^{low}, lower working heat of combustion; X, mass concentration of the gas; η, completeness of combustion; F_c, area of the open surface of the combustible material; a_c, length of the fire load; Bu, Bouguer number; L_{CO} and L_{CO_2}, specific output of carbon monoxide and carbon dioxide; L_{O_2}, specific consumption of oxygen; W, optical density of the smoke; σ_r, Stefan–Boltzmann constant; n, normal to the surface; H_{open}, height of the opening; H_{zone}, height of the critical zone; Φ_{dis}, dissipation function; d, diameter; C_1, C_2, σ_k, σ_ε, and C_μ, constants; d_c, diameter of the combustion site; $f = \dfrac{\delta^{**}}{w_x}\dfrac{\partial w_x}{\partial x}$, form parameter of the boundary layer; δ^{**}, momentum thickness of the boundary layer; $Re^{**} = w_x\delta^{**}/\nu$, Reynolds number; M, mass. Subscripts: sp, specific parameters; ent.a, air entering the building; fl.g, gases flowing outward; stab, stabilization of combustion; 0, parameters at the initial instant of time; eff, effective values of the parameters; c, combustible material; open, open opening; x, y, and z, projections on the coordinate axes; t, turbulent; r, radiative heat transfer; i and j, projections on the coordinate axes differing from each other; d, diffusion; zone, parameters of the critical zone; m, mass.

REFERENCES

1. *Information on Emergencies in the Territory of the Russian Federation in 1999*, in: *Problems of Safety under Emergency Conditions* [in Russian], Issue 2 (2000), pp. 234–238.
2. V. L. Ginzburg, *Usp. Fiz. Nauk*, **169**, No. 4, 420–441 (1999).
3. S. V. Pusach, *Inzh.-Fiz. Zh.*, **73**, No. 3, 621–626 (2000).
4. S. V. Pusach and V. G. Pusach, *Inzh.-Fiz. Zh.*, **74**, No. 1, 35–40 (2001).
5. S. Patankar, *Numerical Methods for Solving Problems of Heat Transfer and Dynamics of Fluid* [Russian translation], Moscow (1984).
6. L. G. Loitsyanskii, *Mechanics of Liquids and Gases* [in Russian], Moscow (1990).
7. M. N. Ozisik, *Combined Heat Transfer* [Russian translation], Moscow (1976).
8. V. M. Astapenko, Yu. A. Koshmarov, I. S. Molchadskii, and A. N. Shevlyakov, *Thermogasdynamics of Fires in Rooms* [in Russian], Moscow (1986).
9. A. V. Gomozov, *Study of the Boundary Conditions of Heat Transfer for Calculation of Fire-Proof Plane Horizontal Structures under Fire Conditions*, Candidate's Dissertation (in Engineering), Moscow (1983).
10. M. Ya. Roitman, *Fire-Fighting Normalization in Civil Engineering* [in Russian], Moscow (1985).
11. S. I. Zernov, *Development of Computational Techniques for Prediction of the Parameters of Fires in Rooms of Buildings with Natural Ventilation*, Candidate's Dissertation (in Engineering), Moscow (1984).
12. S. V. Pusach, *Thermophysical Principles of Fire- and Explosion Safety in Hydrogen Power Engineering*, Doctoral Dissertation (in Engineering), Moscow (2000).
13. S. V. Pusach, *Inzh.-Fiz. Zh.*, **72**, No. 5, 1025–1032 (1999).
14. S. V. Pusach and R. V. Prozorov, in: *Problems of Safety under Emergencies* [in Russian], Issue 7 (1999), pp. 122–127.
15. Yu. A. Koshmarov, *Prediction of Hazardous Factors of Fire in Rooms: Textbook* [in Russian], Moscow (2000).
16. S. V. Pusach, V. G. Pusach, and R. V. Prozorov, in: *Proc. IV Minsk Int. Forum "Heat and Mass Transfer–MIF-96"* [in Russian], Vol. 3, 22–26 May 2000, Minsk (2000), pp. 340–347.